Chapter 13
Printed Anisotropic Molecular Alignments

Munehiro Kimura

Abstract The fabrication of ordered organic molecular layers is of fundamental interest in many opto-electronic applications. Needless to say, the performance of liquid crystal displays, organic light emitting devices, organic field effect transistors and organic photovoltaic cells all depends on achieving a required degree of molecular alignment. To date, several processes have been developed to achieve the alignments, including the rubbing, Langmuir-Blodgett, alignment transcription, flow coating, gravure coating, and slit coating methods. In this chapter, these fabrication methods will be introduced and discussed and future technologies will be considered.

13.1 Necessity of Controlling Molecular Alignment and Demand for Printing Techniques

At present, liquid crystal displays (LCDs) are among the most successful organic electronic devices [1, 2]. The basic operation of LCDs is made possible by the reorientation of liquid crystal (LC) molecules that are initially aligned in a certain direction using a so-called alignment film. One of the most important performance indices associated with LCDs is the so-called contrast ratio, defined as the ratio of maximum to minimum luminance. Light leakage in the extinction state (equal to the minimum luminance) resulting from imperfect alignment of the liquid crystal molecules deteriorates this contrast ratio, meaning that the initial molecular alignment is the most vital factor affecting LCD quality. Molecular alignments near boundary surfaces have been widely studied on the basis of both experimental and theoretical aspects and there have been many reports on LCDs that discuss the nature of their molecular alignment and means of controlling this alignment [3, 4].

M. Kimura (✉)
Department of Electric Engineering, Nagaoka University of Technology, 1603-1 Kamitomioka, Nagaoka 940-2188, Japan
e-mail: nutkim@nagaokaut.ac.jp

Q. Li (ed.), *Anisotropic Nanomaterials*, NanoScience and Technology,
DOI 10.1007/978-3-319-18293-3_13

The mechanical rubbing method is still widely used for industrial purposes, since it is readily applicable to mass-production. Recently, however, the patterned photo-alignment technique has been put into practical use. In general, all LC alignment techniques are in many ways similar since the LC must in all cases exhibit orientational order and the capacity for self-assembly. The role of the alignment film when fabricating LC devices is to promote the initial alignment of the LC molecules.

The alignment of organic semiconductors in optoelectronic and electronic devices can be considered analogous to the alignment of LC molecules in LCDs. In the case of an organic semiconductor, charge transport can be attributed to π-bonding orbitals and quantum mechanical wavefunction overlaps, and so a molecular order that enhances the π-bonding overlap between molecules is important [5, 6]. It has been reported that the carrier mobility in field-effect transistor devices consisting of pentacene nanolayers is remarkably improved by inserting a self-assembled monolayer (SAM) at the semiconductor/gate dielectric interface [7]. This enhanced mobility can be explained by the formation of large, highly π-conjugated crystal grains in the pentacene nanolayers formed at the SAM surface. That is, the SAM assists in the molecular alignment of the pentacene.

The requirements for future applications of organic electronic devices such as LCDs and organic semiconductor devices, including organic thin film transistors (OTFTs), organic light emitting diodes (OLEDs) and organic photo voltaic (OPV) devices, are similar: bendability (or flexibility) and printability. These applications, sometimes referred to by the general term printed electronics, have significant potential to allow new innovations in electronic devices [8]. To promote the practical applications of these organic electronic devices, the development of molecular alignment techniques is quite important. In the following sections, molecular alignment techniques with applications to the formation of LCDs are reviewed, including a brief discussion of conventional techniques such as rubbing, for which it should be emphasized that an alignment film is required. In addition, novel alternative techniques such as gravure printing and slit coating that do not require preparation of an alignment film are introduced.

13.2 LC Alignment by Means of an Alignment Film

In general, LC molecular alignment is accomplished by means of a polymeric alignment film, which is first applied to a substrate and then treated in some manner. In industrial applications, polyimide derivatives are widely used for this purpose and may be treated using the gravure coating method, as shown in Fig. 13.1. Following this treatment, the film functions as an alignment film.

The mechanical rubbing method, first reported by Mauguin in 1911, is one of the most common means of processing the polymeric alignment film [9]. Figure 13.2 presents an illustration of a typical rubbing machine. As its name suggests, the surface of a polymeric film previously applied to the substrate is mechanically

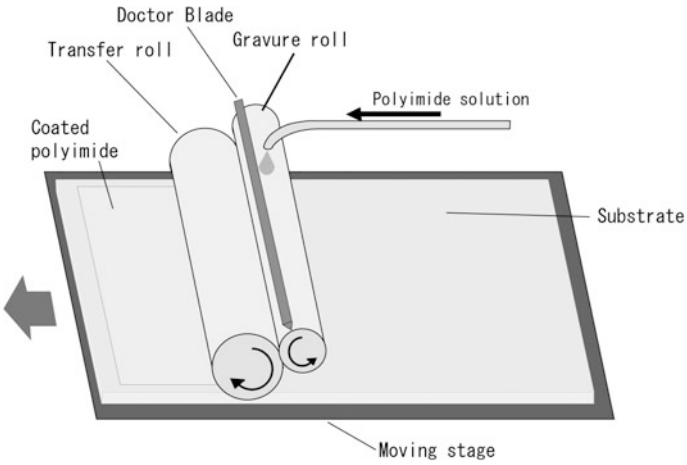

Fig. 13.1 Gravure coater for coating polyimide alignment film

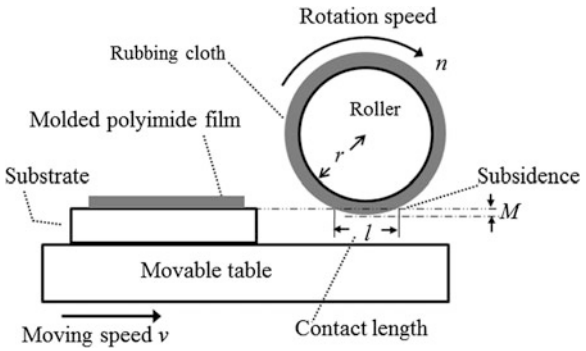

Fig. 13.2 Schematic illustration of a rubbing machine

rubbed by a cloth wrapped around a drum. The untreated polymer film has no alignment capability but is capable of inducing LC alignment following the rubbing process. The rubbing process is fairly practical, although the associated mechanism by which rubbing enhances the film and the action that the rubbed polymer film exerts to generate LC molecular alignment are not perfectly understood. It can be said, however, that mechanically-induced anisotropy on the alignment film surface induces an anisotropic interaction with the LC molecules [10–12].

As noted, the anisotropy in the treated alignment film results in LC alignment and, to date, several alternative methods for introducing anisotropy in the film have been proposed. In 1987, Kakimoto et al. reported that Langmuir-Blodgett (LB) films of polyimides deposited on a substrate exhibited a fair degree of orientation relative to the transfer direction of the substrate [13]. Figure 13.3 illustrates the LB method, also known as the vertical dipping method. These deposited LB films

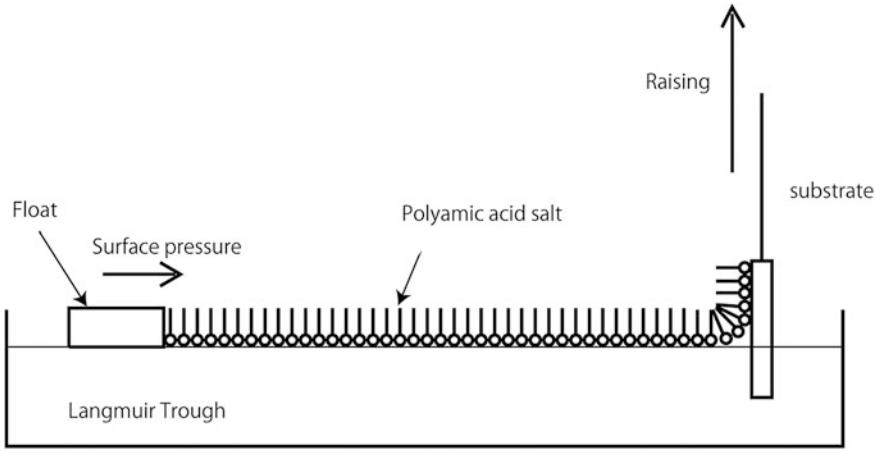

Fig. 13.3 Schematic illustration of Langmuir-Blodgett method. Substrate is moving upward and downward in order to move the monomolecular polyamic acid salt film from the water surface. This method is also called vertical dipping method

exhibit the ability to induce planar LC alignment without rubbing. A mechanism by which LC alignment is induced by LB films has been suggested [14], in which a polymeric LB film transferred onto a substrate by upwards pulling perpendicular to the water surface is stretched uniaxially, generating anisotropy. Mechanical stretching, however, is not the only external influence that induces anisotropy; the photo alignment method is one of the promising techniques from an industrial standpoint [15].

13.3 Surface Memory Effect

It is important to note that, in the abovementioned LCD preparation methods, the polymeric film must be preprocessed by external stimuli before applying the LC molecules. Some unique experiments have demonstrated that alignment may also be accomplished by taking advantage of the memory effect [16–18], by which "LCs align LCs" [19] thus maintaining orientational order. In the case of organic field effect transistors (OFETs), it is important to develop deposition techniques capable of simultaneously aligning the crystal axes, so as to induce enhanced mobility, and increasing the crystalline grain size, such that it is larger than the channel length of the OFET. Many methods have been proposed for producing organic semiconductor molecules, including flow coating [20], zone casting [21], drop casting on tilted substrates [22], hollow-pen writing [23], solution-sheared deposition [24], sustaining of a semiconductor solution on a tilted substrate [25], dip coating [26] and droplet drying under a directional gas flow [27]. In these methods, the

directional movement of the air-solution-substrate contact line (i.e. the shear flow force) is usually the driving force aligning the organic molecules. Once an external force is applied to the molecules, the molecular alignment is sustained through their recrystallization from that starting structure, especially near the substrate surface. Of these methods, we will examine the alignment transcription, reactive mesogen polymerization and flow-coating methods, since these lead to the development of the alignment printing methods described further on.

13.3.1 Alignment Transcription Method

Toko et al. proposed a non-rubbing technique known as the alignment transcription (AT) method [28], involving the fabrication processes shown in Fig. 13.4. Here the original substrates are coated with pre-rubbed polyimide films while the counter

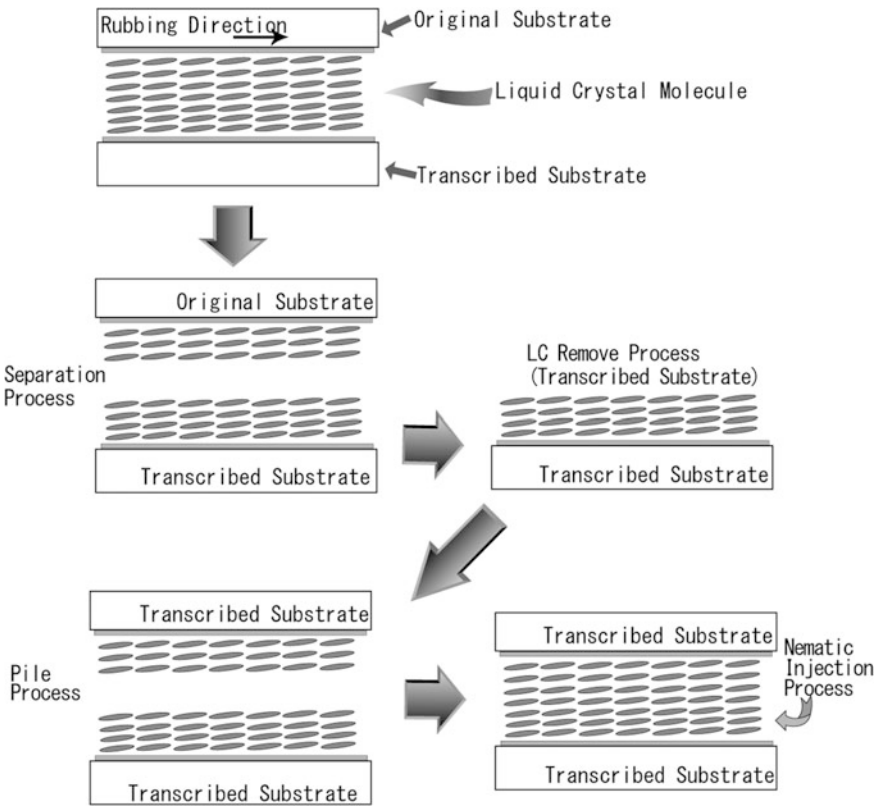

Fig. 13.4 Fabrication processes of the Alignment transcription method. Reproduction by permission from [28]

substrates are coated with non-rubbed polyimide films. An original substrate is placed upon a transcribed substrate, leaving an appropriately-spaced gap, to make the transcription cell, and then heated to the temperature at which the LC exhibits its isotropic phase, to allow for LC injection. The cell is subsequently cooled to ambient temperature, whereupon the LC transitions to the nematic phase and LC molecules are aligned along the rubbing direction of the original substrate. The original substrate is then separated from the transcribed substrate, removing all the LC molecules except for those situated in the vicinity of the surface of the transcribed substrate. Finally, the transcribed substrate is placed over another transcribed substrate to form an AT-LC cell and the LC in the nematic phase is injected into this cell. The azimuthal anchoring strength of the AT-LCD process has been reported to be comparable to that obtained by the rubbing process, suggesting that the LC molecular order propagated from the bulk orientation can be memorized by the polyimide surface. Unfortunately, due to the labor-intensive repetitive cell fabrication process involved with this technique, the AT method has not been put into practical use.

13.3.2 Polymerization of a UV-Curable Reactive Mesogen Monomer at the Surface

To obtain high image quality with LCDs, the patterned vertical alignment (PVA) mode is typically used [29]. In a PVA panel, the pixel and common electrodes are situated in an alternating pattern and thus an oblique field having vertical and horizontal components is generated, with a biased applied voltage that rotates the LC molecules downwards in four different diagonal directions. Challenges associated with the real-applications of LCDs to the PVA mode included unexpected disinclination and insufficient response time, especially when the applied electric voltage is kept low so as to maintain a low gray level. Furthermore, additional structures such as protrusions are required. Kim et al. has proposed a relatively simple technique to solve these problems that requires neither the rubbing process nor protrusion structuring [30]. In this method, a UV-curable reactive mesogen (RM) monomer and a photoinitiator are doped into the nematic LC mixture in advance. The mixture is placed in the PVA cell, the inner surfaces of which have a vertical alignment layer with patterned electrodes, as shown in Fig. 13.5. Immediately following LC injection, the RM monomer and the LC molecules are vertically aligned. Subsequently, a voltage higher than the Freedericksz transition voltage (V_{th}) is applied to the cell such that the RM monomer as well as the LC reorient at a slight tilt angle from the vertical alignment in response to an electric field. In this state, the PVA cell is exposed to UV light, during which the RM monomers are polymerized at a constant tilt angle on the surface of the substrate and thus a pretilt layer is formed in the cell and remains in this state even after removing the voltage. Using this process, the pretilt angle can be controlled on the

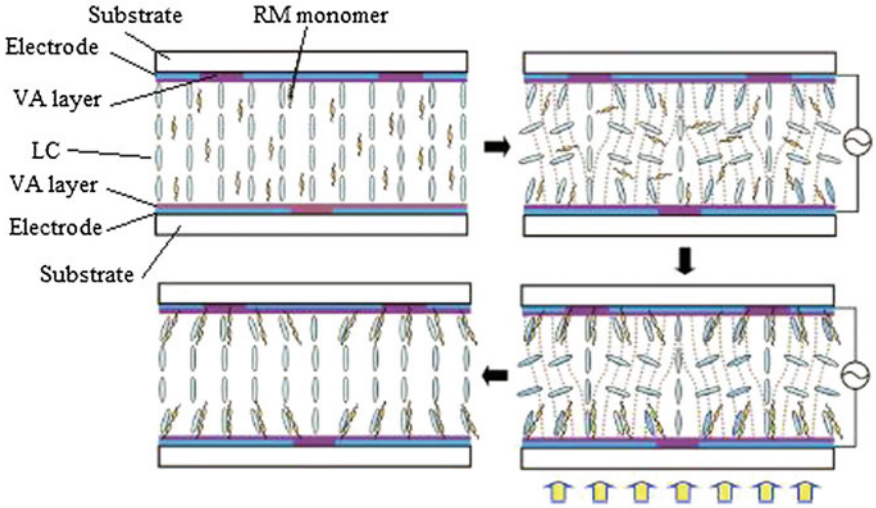

Fig. 13.5 Schematic illustration of the patterned vertical alignment (PVA) cell exhibiting how the pretilt angle is formed using reactive mesogen (RM) monomer. Reproduction by permission from [30]

surface of a vertical alignment film and, as a result, the necessary driving voltage and response time are both reduced. Recently, a technique of this sort not requiring a polyimide film has been proposed [31]. This is possible because the polyimide film is no longer necessary if the RM brings about surface segregation and polymerization in the vicinity of the glass surface, meaning that the polymerized RM film can take the place of the polyimide, such that the surface memory effect acts as a surface anchoring effect.

13.3.3 Flow-Coating Method

It has been reported that a flow-coating method [32] may be useful as a means of forming highly oriented and fairly uniform organic semiconductor material films from materials such as 6,13-bis(triisopropylsilylethynyl) pentacene (TIPSPEN), even on OFET device substrates with pre-deposited source/drain electrodes [20]. This method is understood by considering the work of Sakamoto et al. [20], and Fig. 13.6 shows a schematic illustration of the flow-coating technique. Here the flow coater consists of a movable blade composed of a 13 mm-wide, 2 mm-thick fluorine-coated glass plate, together with a stationary sample stage. The movable blade is inclined at an angle of approximately 1.5° from the substrate surface plane, and the gap height between the blade and the substrate surface is set to 200 μm. After placing the leading edge of the movable blade above the coating start line, 16 μl of a 0.6 wt% solution of TIPSPEN in chloroform is transferred into the blade/substrate gap by

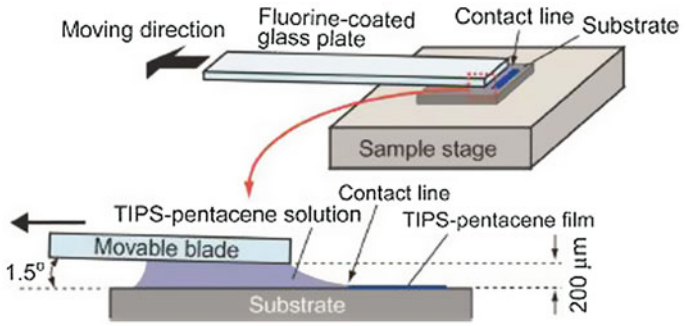

Fig. 13.6 Schematic illustration of the flow-coating method. Reproduction by permission from [20]

capillary action and the flow-coating is immediately initiated at a constant blade speed of 200 µm/s. The flow-coated films thus formed are composed of arrays of needle-shaped crystals whose long axes are aligned along the flow-coating direction. It has been reported that the contact resistance, as well as the field-effect mobility, of bottom-contact/bottom-gate (BC/BG) type TIPSPEN OFETs vary with the channel current direction with respect to the flow-coating direction.

13.4 Printing Methods

All of the methods described above require an auxiliary polymeric film to align the LC molecules, such as a polyimide acting as an alignment film. Such films, however, are no longer necessary if the LC molecules are able to align themselves autonomously. This is advantageous since it obviates the need for the thermal curing step, allows the manufacturing processes to be performed at room temperature and permits plastic rather than glass substrates, all of which reduce production costs. Below, two methods aimed at introducing a printing process are introduced, in particular the slit coating method, which will be described in detail. If and when these coating methods are put to practical use, it is expected that injection-free processes will be possible and productivity will consequently be improved. As noted, these methods are also advantageous since they lower the cost of LCD fabrication by removing the need for an alignment film.

13.4.1 Gravure-Coating Method

As discussed, the standard industrial LCD manufacturing process employs a polyimide alignment film. Such films are commonly treated using the gravure

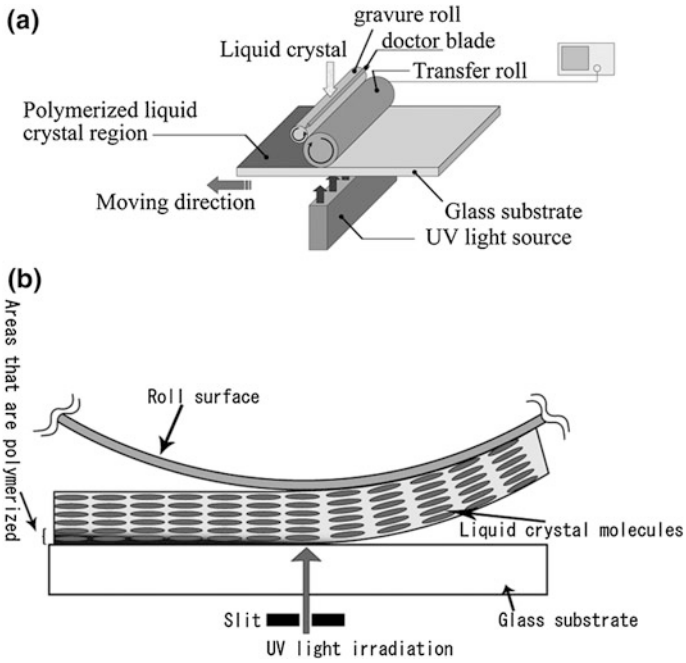

Fig. 13.7 LC gravure printing method. **a** Schematic illustration of the instrument. **b** Model of the LC alignment transfer

coating method and, based on this technique, a novel means of transferring LC molecules that have been aligned in advance has been devised. This process takes advantage of the observation that the substrate need not be flat if sufficient transferring time is allowed. Figure 13.7 illustrates an example of the gravure printing method [33, 34], in which the host LC (ZLI-2293) is doped with a guest UV-curable LC (UCL-011-K1, DIC) acting as the RM. Here the LC molecules are placed between the gravure roll and the doctor blade, following which an LC layer of the desired thickness is formed on the transfer roll. Throughout this process, the linear velocity of the substrate and the rotational speed of the transfer roll are synchronized. The LC molecules are pre-aligned on the transfer roll since the roll is equipped with interdigitated electrodes capable of inducing planar alignment. In the case of vertical alignment, a planar electrode is employed to generate a vertical electric field between the transfer roll and the substrate. The aligned LC molecular layer is subsequently transferred to the glass substrate while maintaining molecular alignment and, immediately following this transfer, the added RM is polymerized by UV irradiation, since otherwise the LC alignment on the glass substrate will be rapidly disrupted by thermally induced motion. It has been reported that UV polymerization of the RM tends to induce surface segregation [35]. That is, the RM is found in higher concentrations in the vicinity of the glass-LC layer interface. It is also important to emphasize that the LC molecules near the air-LC layer interface

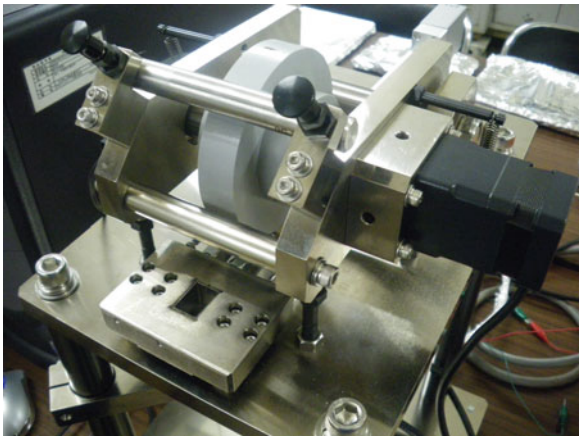

Fig. 13.8 Photograph of the prototype LC gravure coating machine

are not polymerized and remain in the nematic phase because the radical polymerization of the RM is disturbed by atmospheric oxygen. Finally, the LC layer transferred to the substrate is laminated against another LC-transferred substrate to form a sandwich-type LC cell. Figure 13.8 presents a photograph of a prototype LC gravure coating machine. The size of the layer and the LC alignment depend on the printing plate, and therefore multi-domain pattern alignment is also possible with such devices.

13.4.2 Slit-Coater Method

A slit coater, also known as a dye coater or a lip coater, is widely used for painting or spreading a fluid with uniform thickness. Recently, we reported that the slit-coater method is also applicable to LCD fabrication. The slit coater does not merely take the place of the one-drop fill (ODF) process in LCD fabrication; it has been demonstrated that LC layers formed by a slit coater exhibit uniaxial alignment and that this alignment is maintained following UV polymerization, suggesting the possibility of a molecular alignment technique incorporating a non-thermal curing process. In such a process, locally polymerized LC regions would replace the (typically polyimide) molecular alignment film. As a result, a slit coater can potentially serve as both an LC filling process and a molecular alignment process, thus reducing the required quantity of LCD fabrication steps.

Figure 13.9 shows a slit-coater system and a schematic diagram of such a system, including the slit nozzle and UV light source. In this process, the substrate —positioned on the carrier stage—is moved such that it is coated on one side with LC molecules. During this coating, the LC molecules undergo self-organized alignment resulting from the shear-flow force. UV irradiation from the bottom side of the substrate is performed simultaneously to polymerize a thin LC layer adjacent

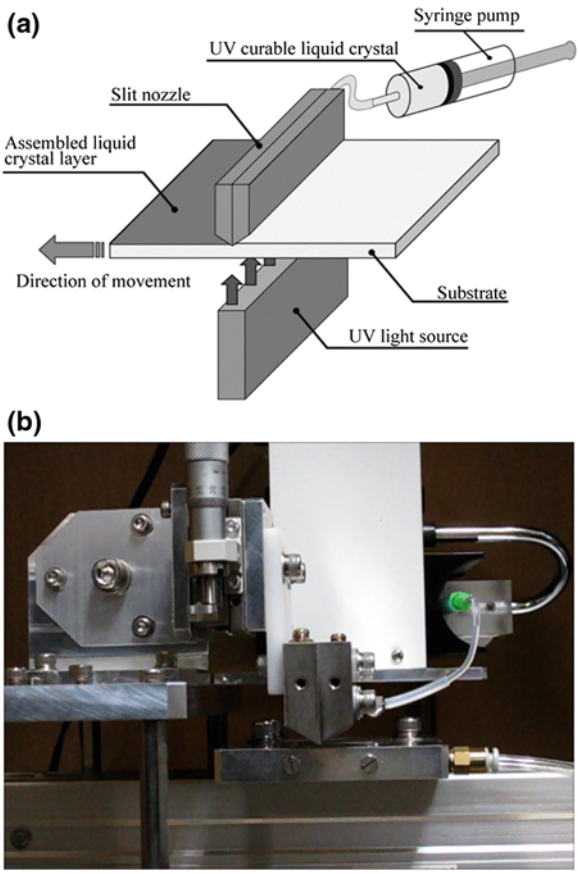

Fig. 13.9 **a** Schematic illustrations of the slit coater method. **b** Photograph of the experimental instrument

to the substrate, as illustrated in Fig. 13.10. This locally polymerized LC region, with a typical thickness of several tens of nanometers, acts as a molecular alignment film. Consequently, the slit coater can be used to achieve both LC filling and molecular alignment. Following the LC coating and UV irradiation, the top surface of the LC layer remains in the nematic phase. Therefore, by combining two such substrates coated in this manner with LC layers, an LCD panel can be fabricated without the LC injection process. As noted, the LC alignment is brought about by the shear flow between the slit nozzle and the substrate. The process parameters that control the LC alignment are therefore the slit width, slit length, coating gap, delivery rate of LC materials from the slit nozzle, stage movement velocity and UV irradiation intensity. In our own experimental trials, the slit width was fixed at 20 μm, the slit length at 13 mm and the coating gap at approximately 100 μm. The LC host molecule was a nematic cyanobiphenyl compound (ZLI-2293, Merck) exhibiting positive dielectric anisotropy, while the guest UV-curable LC was UCL-011-K1 (DIC), added at a concentration of 5 wt%. The LC mixture was delivered to the slit nozzle at a fixed rate using a syringe pump and the stage

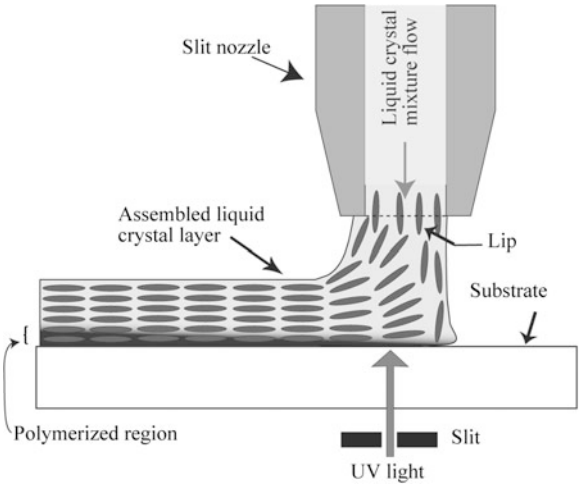

Fig. 13.10 Schematic model of shear flow molecular alignment during the slit coating process

was moved at a fixed rate using a stepper motor. A high pressure Ushio SP9-250DB mercury lamp with a central wavelength of 365 nm was employed as the light source. The stage was moved at 0.50 mm/s and the UV irradiation intensity was 100 mW/cm^2. It is expected that such polymerized thin LC layers will function as well as conventional alignment films.

Figure 13.11a, b present photographs of the coated LC films, in which the coating direction is parallel to the crossed polarizer (a) and at 45° with respect to the polarization axis of one polarizer (b). These images show uniform and uniaxial alignment of the layers. Figure 13.12a, b show enlarged images of these same samples obtained by polarized optical microscopy (POM). It is evident that the extinction direction is parallel to the coating direction of the LC layer, suggesting a uniaxial planar alignment of the LC direction. It is also obvious that numerous streak-like defects are present, almost parallel to the LC coating direction. These appear to represent damage to either the LC layer or the substrate, possibly generated mechanically by contact between the slit nozzle and the substrate. To reduce the number of these defects, precise control of the gap between the slit nozzle and the substrate is required. Unfortunately, relatively large gaps on the order of 200 μm generate few defects but also allow for insufficient LC alignment. In Fig. 13.12b, scale-like defects are also found, possibly caused by the movement of the stage. In order to reduce the number of these defects, it was necessary to construct an LC coating system with very precise mechanical movements. For this purpose, a prototype slit coater specially designed for LC alignment was manufactured, as shown in Fig. 13.13 (produced by the Toray Engineering Co., Ltd., Japan). Figure 13.14 presents a photograph of a coated LC film obtained by means of this prototype slit coater, using a slit length of 100 mm, a slit width of 20 μm and a coating gap of approximately 100 μm. The thickness of the coated LC layer is approximately 1 μm. It can be seen that the initial portion of the LC coating, where the slit nozzle first approaches the substrate, is not well aligned, since the molecular

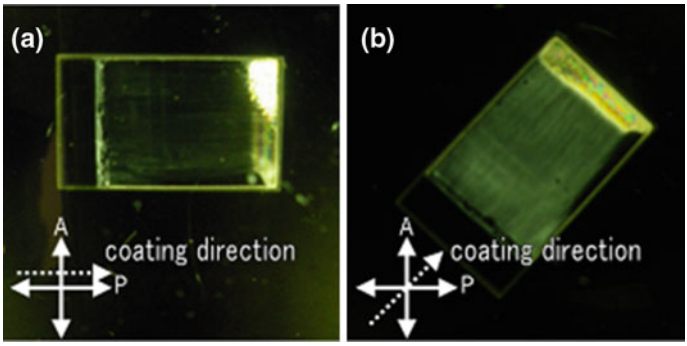

Fig. 13.11 Photographs of the LC films fabricated using the slit coater and simultaneous UV irradiation. **a** The coating direction is parallel to the polarizer under the crossed-nicols. **b** The coating direction is 45° with respect to the polarizer under the crossed-nicols

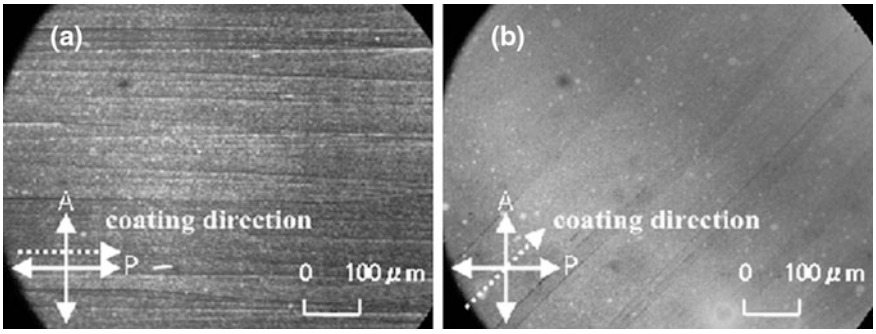

Fig. 13.12 Microphotographs of the LC films fabricated by the slit coater. **a** The coating direction is parallel to the polarizer under the crossed-nicols. **b** The coating direction is 45° with respect to the polarizer under the crossed-nicols

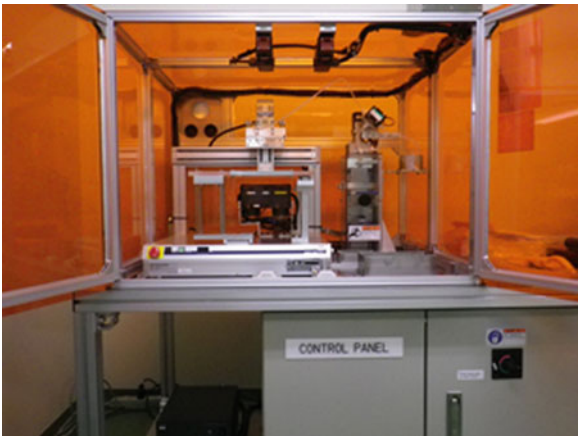

Fig. 13.13 Photograph of the prototype slit coater specialized for LC alignment

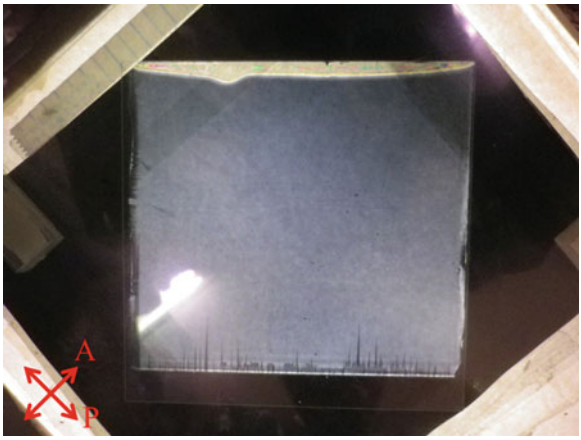

Fig. 13.14 Photograph of the LC alignment fabricated by prototype slit coater. The size of the glass substrate is 100 × 100 mm. The coating direction is 45° with respect to the polarizer under the crossed-polarizers

alignment is difficult to control during the initial discharge from the lip of the nozzle. This effect is currently unavoidable and, in fact, the same defect is seen at the terminal region of the film because no shear flow force is generated around the initial and terminal portions. However, this is not an insurmountable problem; for example, in the case of a roll-to-roll process, the initial and terminal portions of the substrate film could simply be cut off.

As noted, it is assumed that the LC alignment is brought about by the shear flow between the slit nozzle and the substrate. Figure 13.15 presents a numerical simulation of liquid flow based on the Navier–Stokes equation [36], as obtained using commercially available software (ANSYS Fluent, ANSYS Inc.) [37]. In computational fluid dynamics, the semi-implicit method for pressure linked equations (SIMPLE) algorithm is a widely used numerical procedure to solve the Navier–Stokes equation [38]. Here the Navier–Stokes equation was discretized using the finite volume method and, to simplify the calculations, an isotopic liquid with a viscosity of 160 mPa s was assumed, even though the LC is actually an anisotropic fluid. The calculation parameters were as follows: an LC layer thickness of 2 μm, a gap between the lip and the substrate of 100 μm, a contact angle between the substrate and the fluid of 30°, a contact angle between the lip and the fluid of 60°, a surface tension of 30 mN m and a substrate velocity of 10 mm/min. Figure 13.15a shows the shape of the fluid bead between the slit coater lip and the substrate, from which it can be determined that the meniscus front and back radii are approximately 0.2 and 0.3 mm, respectively. Figure 13.15b pictures the fluid pathways, indicating the movement of the fluid over a certain duration of the reduced time. The pathline along the nozzle depicts the fluid flow of the upper LC layer, representing the LC molecules that reach the surface of the bead (the interface between the air and fluid) and that have a relatively low flow velocity. In contrast, the line running directly toward the substrate depicts the fluid flow of the lower LC layer, for which the flow velocity is relatively high. It is evident that there is a distribution of flow velocities between the lip and substrate, and this distribution induces the shear flow.

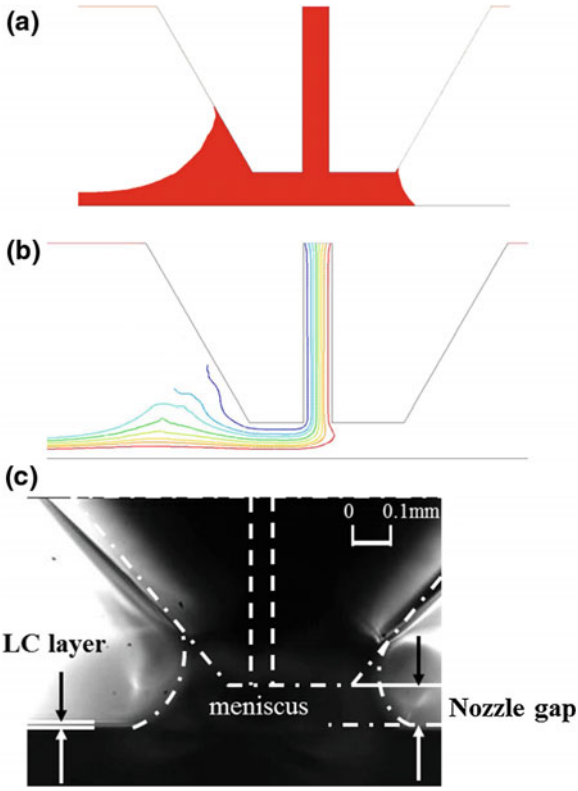

Fig. 13.15 The aspect of the shear flow. **a** Simple numerical simulation of a liquid flow based on the continuity equation and Navier–Stokes equation. **b** Pathlines of the fluid, which represents the trace of the fluid in certain duration of the reduced time. The line color represents the reduced position. **c** High-speed camera snapshot around the lip of slit coater

Figure 13.15c shows a photographic image of the lip of the slit coater obtained with a high-speed camera (Fastcam MC2.1, Photron) during a trial in which a nematic mixture composed of a fluorinated derivative was used. Comparing Figs. 13.15a, c, it is clear that the shape of the bead as captured by the high-speed camera is similar to that depicted by the numerical simulation. Although the dynamics of an anisotropic fluid such as a nematic LC are complex, the gradient of the flow velocity in the numerical simulation suggests the existence of shear flow near the substrate, which induces the LC molecular alignment.

Various investigations were performed with regard to UV irradiation of these layers. In those cases in which the LC alignment is fixed by UV irradiation after the LC coating process is complete, as in Fig. 13.16, it is not necessary to situate the UV source immediately below the slit nozzle and so the LC coating and UV irradiation may be carried out separately. This is beneficial since it prevents the slit nozzle from being covered by the polymerization agent. Furthermore, it is not necessary to synchronize the stage velocity and UV irradiation duration. In trials performed by our group, the UV irradiation intensity was 10 mW/cm^2, the irradiation time was 300 s and the UV light impinged on the sample vertically, coming from the underside of the substrate. Figure 13.17 provides photographic images of

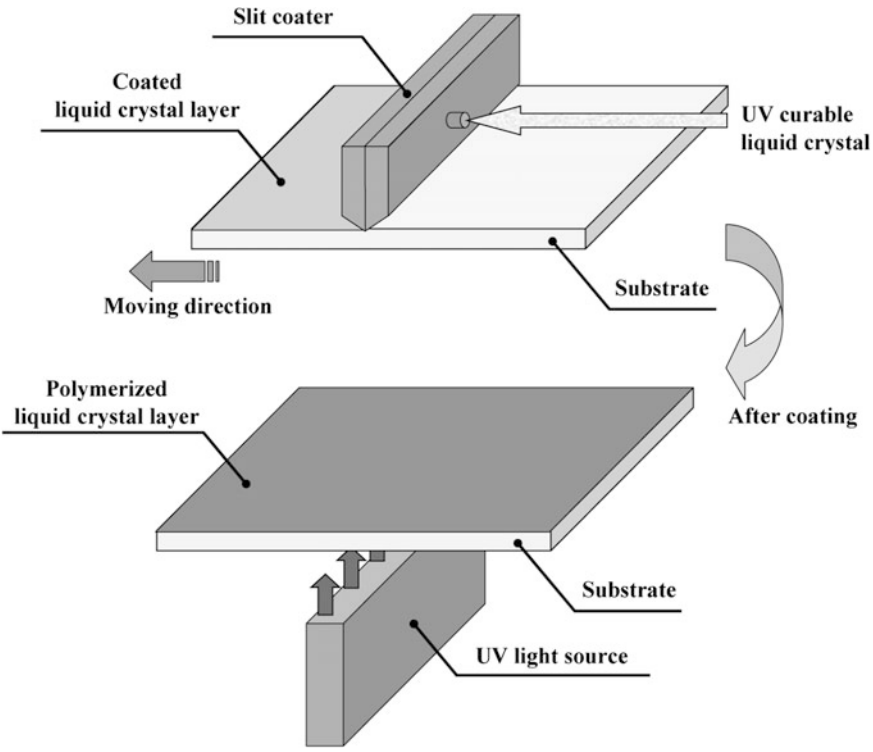

Fig. 13.16 Schematic illustration of the UV irradiation after LC coating using slit coater

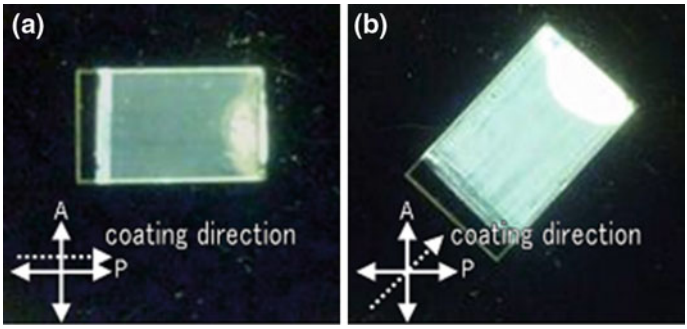

Fig. 13.17 Photographs of LC-coated films consist of ZLI-2293 and UCL-011-K1 before UV irradiation. **a** The coating direction is parallel to the polarizer under the crossed-nicols. **b** The coating direction is 45° with respect to the polarizer under the crossed-nicols

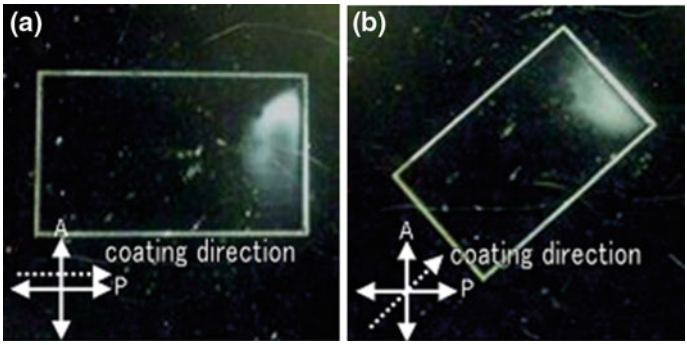

Fig. 13.18 Photographs of LC-coated films consisting of ZLI-2293 and UCL-011-K1 after UV irradiation with high-pressure mercury lamp under crossed polarizer. **a** The coating direction is parallel to the polarizer under the crossed-nicols. **b** The coating direction is 45° with respect to the polarizer under the crossed-nicols

coated LC films under crossed nicols immediately after the coating process and prior to UV irradiation, where the guest material is UCL-011-K1 (DIC). These photographs show that uniform and uniaxial LC alignment was obtained. Figure 13.18 shows photographs of these same coated LC films after UV irradiation. The transmittance under crossed nicols is not changed by rotating the LC-coated film, implying that the planar alignment of the LC changes the vertical alignment. It was also confirmed that this alignment transition behavior was affected by the duration of the UV irradiation, which was typically 40 s. One possible cause of such an effect could be thermal fluctuations induced by the irradiation. To verify this hypothesis, a UV band-pass filter was inserted between the UV light source and the substrate in order to filter out the vis-light. However, the alignment transition behavior was still observed. Subsequently, a He–Cd laser (λ = 325 nm, 10 mW) was introduced in place of the high-pressure mercury lamp, whereupon it was found that this alignment transition behavior was observed regardless of the laser intensity. In order to examine the effect of the RM material, LC-coated films in which the guest material was a mixture of RM257 (Merck), C12A and DMPAP (Aldrich) were fabricated, following which UV irradiation was performed using the He–Cd laser. In this case, the alignment transition behavior was not observed regardless of the extent of UV irradiation. From these experimental results, it is believed that the alignment transition behavior results from anisotropic polymerization, which in turn is dependent on the guest material [39].

To allow practical application of the slit coater, it is necessary to consider the structure of the moving stage that acts as the substrate carrier. The motion of the moving stage has to be precise so as to maintain the gap between the substrate and slit nozzle. As shown in Fig. 13.19a, the UV irradiation is carried out through the moving stage and so the stage must transmit UV light and cannot be constructed of metal plate. In our case, the glass substrate was carried on a square frame. Although this is sufficient to carry a small substrate, a larger, thin substrate would likely warp

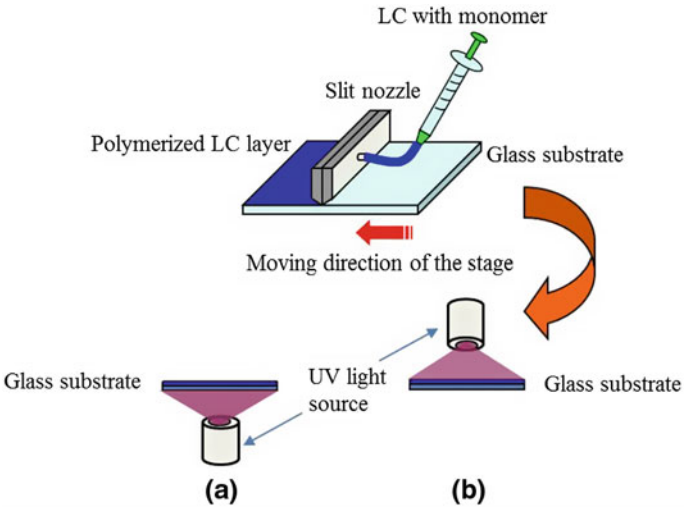

Fig. 13.19 Schematic diagram of the slit coater and UV irradiation. **a** UV irradiation from the side of a glass substrate (exposure type 1), **b** UV irradiation from the side of the air-LC interface (exposure type 2)

under such conditions. Thus, to coat LCs with uniform thicknesses, it is recommended that the moving stage be made of a flat, solid plate with UV light projected downwards onto the LC layer. To assess other potential scenarios, LC layers were polymerized under two UV irradiation conditions; irradiation from the side of the glass substrate (exposure type 1) and irradiation from the side of the air-LC interface (exposure type 2). The effects of UV dosage on the electro-optical (EO) characteristics of LC sample cells fabricated under the two proposed conditions were then assessed. A host nematic LC material (Merck ZLI-2293), a liquid crystalline diacrylate monomer (1.0 wt%, Merck RM257) and a photoinitiator (0.1 wt%, 2,2-dimethoxy-2-phenyl acetophenone, DMPAP, Aldrich) were used in this study. The UV irradiation times were 30 or 90 s and the UV irradiation intensity was set to 5 mW/cm^2, using a deep UV Ushio Spot Cure SP9-250DB lamp at 365 nm. It is known that, even during the early stages of polymerization, the formation of the polymer network is accompanied by the phase separation of the reaction mixture into two regions: polymer-rich and LC-rich [40]. This phase separation results in a solidified polymer film in the region of the substrate closest to the UV source. Therefore, the polymer-rich region will be formed in the vicinity of the substrate in the case of exposure type 1 while, for exposure type 2, the polymer-rich region will be formed near the air-LC interface. These different boundary conditions will have an impact on the voltage-dependent transmittance (V–T) and hysteresis characteristics of the slit-coated twisted-nematic (TN) LC cells. Figure 13.20 presents the V–T curves and hysteresis characteristics of slit-coated TN LC cells fabricated under exposure types 1 and 2 at room temperature. The V–T curves show that, for both types of UV exposure conditions, the average threshold

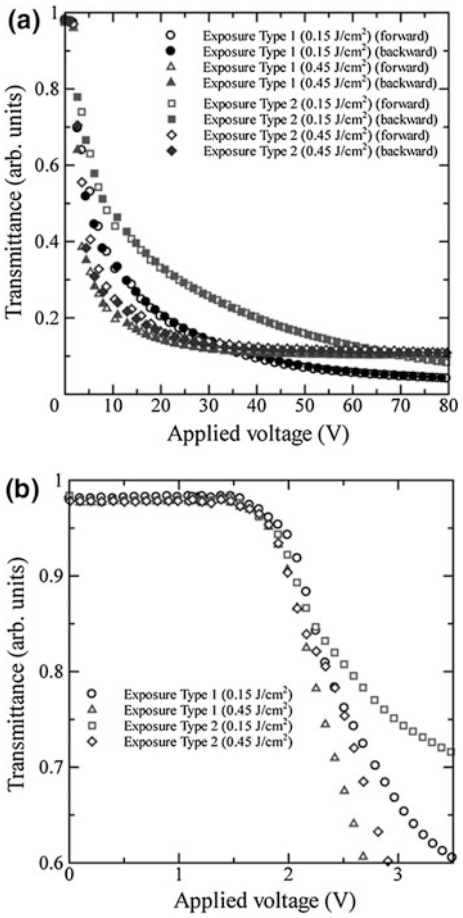

Fig. 13.20 **a** V–T curves and hysteresis characteristics of slit-coated TN LC cells fabricated under exposure types 1 and 2 at UV exposure dosages of 0.15 and 0.45 J/cm^2 at room temperature and **b** V–T curves near the threshold voltages

voltage was ∼1.5 V and the slit-coated TN LC cells could be switched to the black state at rather high voltages. From the V–T curves it is also evident that there was almost no hysteresis behavior. However, effects of the UV exposure type and exposure dosage on the steepness of the V–T curves were observed. These steepness parameter characteristics indicate that exposure type 1 gives steeper V–T curves and that longer exposure times produce steeper curves. The curve steepness for these slit-coated TN LC cells was also found to be greater than those for conventional TN LC cells. It was concluded that the V–T characteristics of cells made using exposure type 2 were inferior to those produced using exposure type 1 [41]. In accordance with these experimental results, plate-like quartz glass was subsequently adopted as a moving carrier stage, as shown in Fig. 13.13.

Figure 13.21 summarizes the dependence of the pretilt angle on the UV exposure dosage [42]. Here higher UV exposures are seen to generate larger pretilt angles on the slit-coated substrate surface. It is believed that increasing UV exposures form a

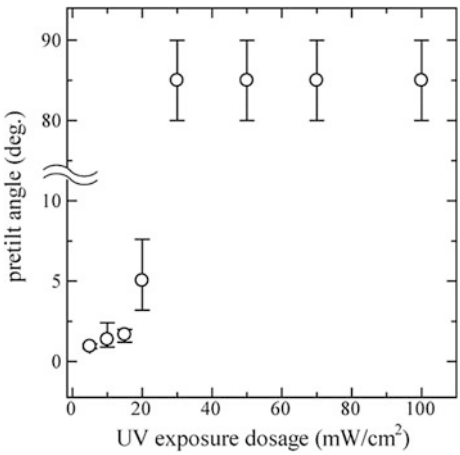

Fig. 13.21 Dependence of the pretilt angle on the UV exposure dosage

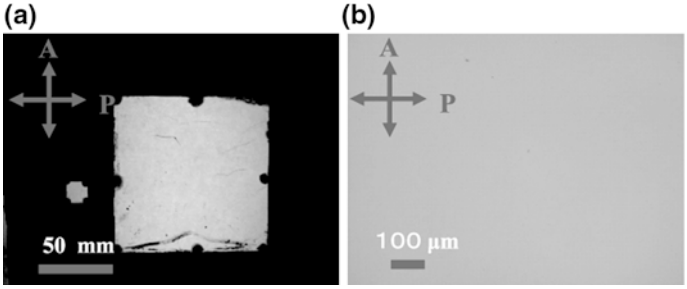

Fig. 13.22 Photographs of the TN-LCD **a** Fabricated by experimental instrument (*left*) and prototype instrument (*right*). **b** Microphotograph of TN-LCD fabricated by prototype instrument

denser polymer network, resulting in a stronger anchoring force sustaining the pretilt of the LC molecules on the substrate surface [43]. These higher pretilt angles are likely due to the surface hydrophobicity of the substrate, as has been reported previously in the literature [44]. The resulting pretilt angle will also depend on the structure and concentration of the RM as well as on the process conditions [45–49].

Figure 13.22 shows photographs of TN LCDs fabricated using the slit-coater method, acquired using the transmission mode (or say normally white mode). As can be seen from these images, sufficiently uniform alignment was realized. Figure 13.23 presents the experimental results for the EO properties of TN LCDs formed using the UV curable additive RM257 at concentrations of 2.1 and 1.1 wt% [37]. For comparison purposes, the same TN LCD was made using the conventional rubbing method, employing a polyimide alignment film. Compared with the reference TN-LCD, similar EO properties were obtained at UV intensities of 5 mW/cm^2, and no hysteresis characteristics are observed in the EO response in Fig. 13.23b.

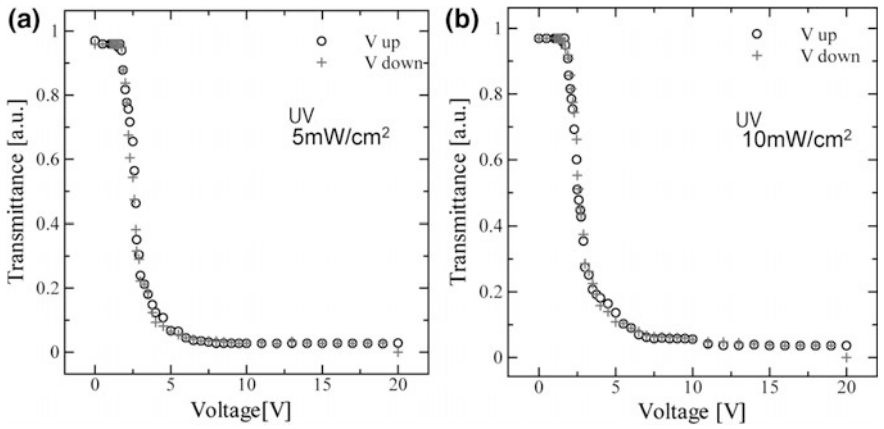

Fig. 13.23 Electro-optical properties of the TN-LCD fabricated by slit coater method. **a** The dosage of RM257 was 2.1 wt%. **b** The dosage of RM257 was 1.1 wt%

Regardless of the UV intensity, the threshold voltage was 1.9 V, which coincides with that for the reference TN LCD fabricated by the rubbing method. The contrast ratio is approximately 84.3, which again is not inferior to that of the LCD made by the conventional rubbing method (approximately 90.4) under laboratory conditions. However, when applying the UV curable additive at 2.1 wt% and/or UV intensities of 10 mW/cm^2, the EO properties below 5 V and above 12 V were different to those of the reference TN LCD. This difference appears to result from variations in the polymer network formation process.

In the revised fabrication process, it is quite beneficial that the production time is only a few minutes from the first substrate washing to the substrate lamination, since the baking process for the alignment film (which typically takes several tens of minutes) is not required. Furthermore, the performance of the TN LCD made using the slit coater method is equal to that of the TN LCD made by the rubbing method. By way of a trial, an in-plane switching (IPS) mode LCD was fabricated on a film substrate. It should be noted that the fabricated IPS-LCD was not a conventional sandwich type LCD but rather a single substrate type LCD not incorporating a counterpart substrate, as shown in Fig. 13.24b. Figure 13.24c shows the appearance of the IPS LCD, for which the driving area was 10 × 10 mm^2. As shown in Fig. 13.24c, a bendable IPS LCD film was obtained, and exhibited completely satisfactory switching operation (white region in the figure). Figure 13.25 presents the experimental results for the EO properties of an IPS LCD fabricated by the slit-coater method, employing UV-reactive mesogens at concentrations of 0.02 wt% (DMPAP) and 0.1 wt% (RM257). This figure demonstrates that the device produced a normal response with minimal hysteresis. In this case, a counterpart substrate was not included and, as a result, the air-LC interface had no anchoring function, which in turned caused the hysteresis in the EO response. In a real LCD,

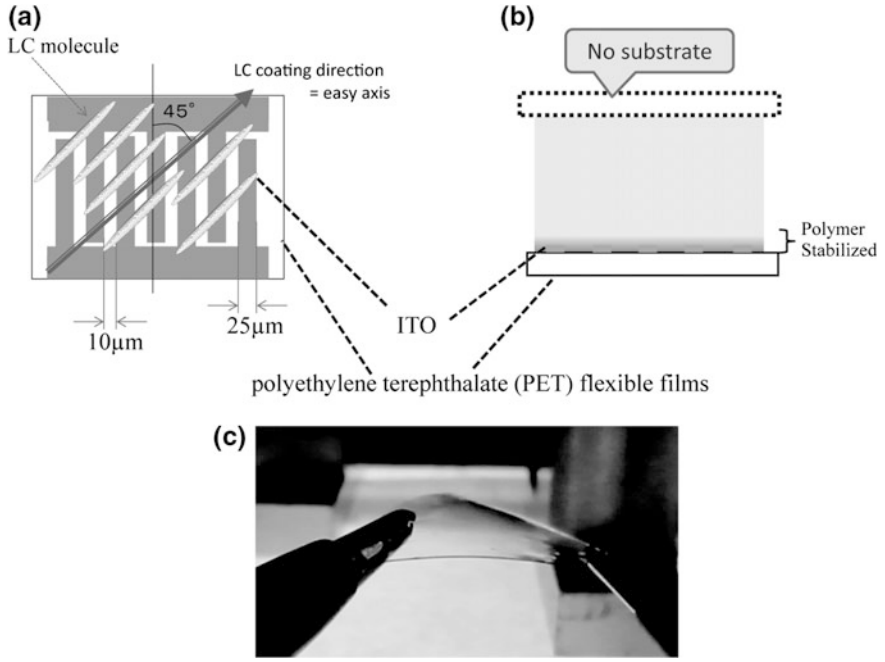

Fig. 13.24 Schematic model of single film substrate IPS-LCD. **a** Top view model. **b** Side view model. **c** Appearance of the IPS-LCD fabricated by experimental instrument

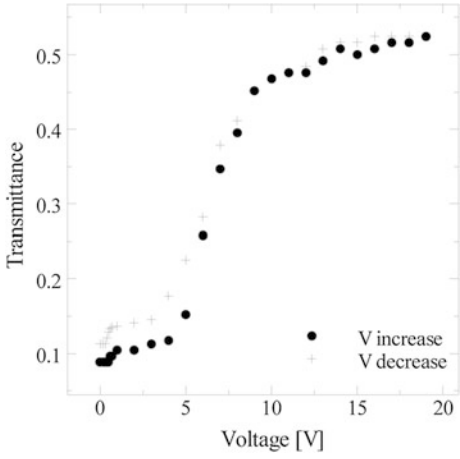

Fig. 13.25 Electro-optical properties of the IPS-LCD fabricated on single substrate

because of the fluidity of the LC, a counterpart substrate would be required. Figure 13.26 shows a sandwich-type, bendable TN-LCD fabricated using a prototype slit coater with polycarbonate films.

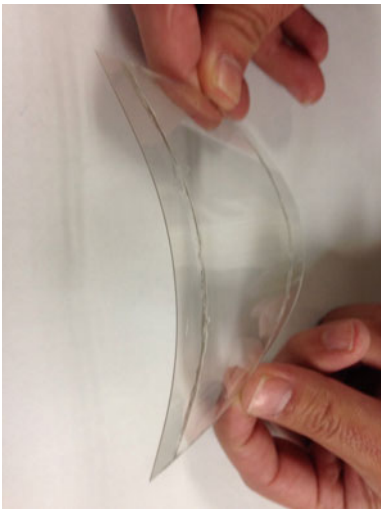

Fig. 13.26 Appearance of the bendable TN-LCD made by polycarbonate films

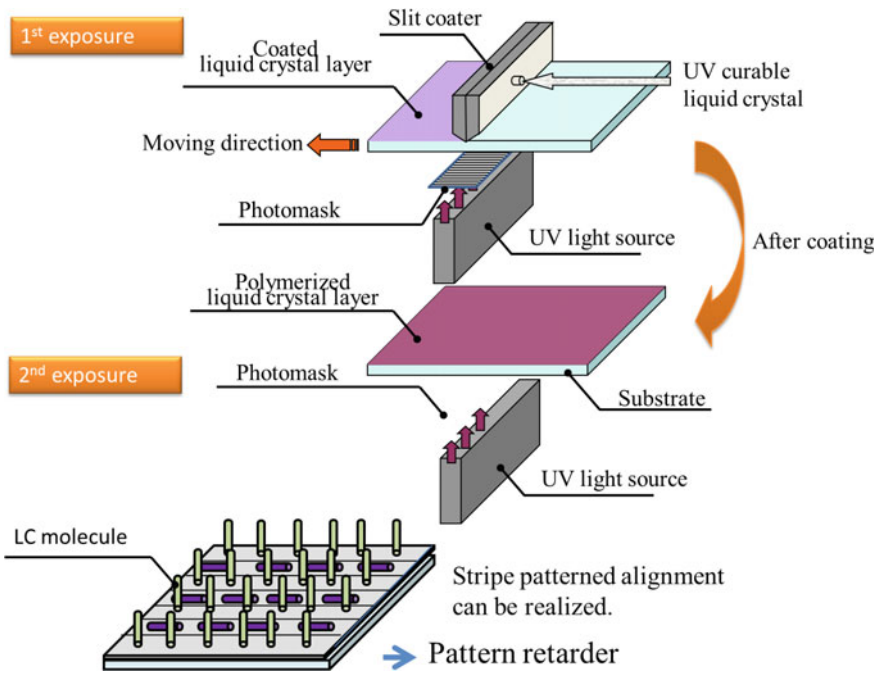

Fig. 13.27 Model of the vertical/planar striped alignment. Firstly, UV irradiation through a grid photomask is carried out in order to polymerize the planarly aligned regions. Then whole the substrate was UV irradiated to reveal the vertical alignment

13.5 Future Applications of the Printing Method

Rather than high quality, so-called "printed electronics" are more often expected to offer flexibility, bendability, robustness and low cost. With regard to reducing the manufacturing cost, plastic films have higher potential than advanced glass substrates [50]. In addition, the slit-coater method is adaptable for use with roll-to-roll technology as a continuous production process for LCDs. In the case of nano-imprint lithography, a master mold is required [51] and large master molds are costly and tend to wear away with use. A further advantage of the slit-coater method is therefore the lack of a master mold, since patterned alignment in which the vertical and planar alignments are arranged in an alternating fashion can be realized by inserting a grid photomask, as shown in Fig. 13.27. Useful products that may result from this process are pattern retarders and patterned polarizer films and, in the near future, the use of plastic substrates in conjunction with roll-to-roll processing should allow commercial scale production of leaflet-type, disposable LCDs. The slit-coater method may also be extended beyond the alignment of LCs and applied to the alignment of nano-rods. In addition, certain RM materials may be anisotropically polarized following polarized UV irradiation. Thus a rich variety of commercial products can be predicted to result from these novel technologies.

References

1. E. Lueder, *Liquid Crystal Displays* (John Wiley & Sons, Chichester, 2001)
2. D.-K. Yang, S.-T. Wu, *Fundamentals of Liquid Crystals* (John Wiley & Sons, Chichester, 2006)
3. T. Uchida, H. Seki, Surface alignment of liquid crystals, in *Liquid Crystals-Applications and Uses*, vol. 3, ed. by B. Bahadur (World Scientific, 1990)
4. K. Takatoh, M. Hasegawa, M. Koden, N. Itoh, R. Hasegawa, M. Sakamoto, *Alignment Technologies and Applications of Liquid Crystal Devices* (Taylor & Francis, London, 2005)
5. V. Coropceanu, J. Cornil, D.A. da Silva Filho, Y. Olivier, R. Silbey, J.L. Brédas, Charge transport in organic semiconductors. Chem. Rev. **107**, 926–952 (2007)
6. H. Ishii, K. Kudo, T. Nakayama, N. Ueno (eds.), *Electronic Processes in Organic Electronics* (Springer, Japan, 2015)
7. C.D. Dimitrakopoulos, P.R.L. Malenfant, Organic thin film transistors for large area electronics. Adv. Mater. **14**, 99–117 (2002)
8. K. Suganuma. *Introduction to Printed Electronics*, Springer, 2014
9. C. Mauguin, Sur les cristaux liquides de Lehmann. Bull. Soc. fr. Miner. **34**, 71–76 (1911)
10. J.M. Geary, J.W. Goodby, A.R. Kmetz, J.S. Patel, The mechanism of polymer alignment of liquid crystal materials. J. Appl. Phys. **62**, 4100–4108 (1987)
11. H. Kikuchi, J.A. Logan, D.Y. Yoon, Study of local stress, morphology, and liquid crystal alignment on buffed polyimide surfaces. J. Appl. Phys. **79**, 6811–6817 (1996)
12. I. Hirosawa, Method of characterizing rubbed polyimide film for liquid crystal display devices using reflection ellipsometry. Jpn. J. Appl. Phys. **35**, 5873–5875 (1996)
13. Y. Nishikata, A. Morikawa, Y. Takiguchi, A. Kanamoto, M. Suzuki, M. Kakimoto, Y. Imai, Orientation of polymer chain of polyimide LB films, and alignment of liquid crystals on the LB films. Nippon Kagaku Kaishi **11**, 2174–2179 (1987), Electrooptic bistability and threshold

characteristics of ferroelectric liquid crystal cell possessing polyimide Langmuir-Blodgett film as an aligning layer. Jpn. J. Appl. Phys. **27**, L1163–L1164 (1988)
14. M. Sugi, N. Minari, K. Ikegami, S. Kuroda, K. Saito, M. Saito, Vertical dipping method as a means of controlling the in-plane molecular orientation in Langmuir-Blodgett films. Thin Solid Films **178**, 157–164 (1989)
15. O. Yaroshchuk, Y. Reznikov, Photoalignment of liquid crystals: basics and current trends. J. Mater. Chem. **22**, 286–300 (2012)
16. N.A. Clark, Surface memory effects in liquid crystals: influence of surface composition. Phys. Rev. Lett. **55**, 292–295 (1985)
17. Y. Ouchi, M.B. Feller, T. Moses, Y.R. Shen, Surface memory effect at the liquid-crystal-polymer interface. Phys. Rev. Lett. **68**, 3040–3043 (1992)
18. B.O. Myrvold, A weak surface memory effect in liquid crystal cells with rubbed polyimide layers. Liq. Cryst. **18**, 287–290 (1995)
19. T. Shioda, Y. Okada, D.-H. Chung, Y. Takanishi, K. Ishikawa, B. Park, H. Takezoe, Liquid crystals align liquid crystals. Jpn. J. Appl. Phys. **41**, L266–L268 (2002)
20. K. Sakamoto, J. Ueno, K. Bulgarevich, K. Miki, Anisotropic charge transport and contact resistance of 6,13-bis(triisopropylsilylethynyl) pentacene field-effect transistors fabricated by a modified flow-coating method. Appl. Phys. Lett. **100**, 123301 (2012)
21. A. Tracz, J.K. Jeszka, M.D. Watson, W. Pisula, K. Müllen, T. Pakula, Uniaxial alignment of the columnar super-structure of a hexa (alkyl) hexa-*peri*-hexabenzocoronene on untreated glass by simple solution processing. J. Am. Chem. Soc. **125**, 1682–1683 (2003)
22. W.H. Lee, D.H. Kim, Y. Jang, J.H. Cho, M. Hwang, Y.D. Park, Y.H. Kim, J.I. Han, K. Cho, Solution-processable pentacene microcrystal arrays for high performance organic field-effect transistors. Appl. Phys. Lett. **90**, 132106 (2007)
23. R.L. Headrick, S. Wo, F. Sansoz, J.E. Anthony, Anisotropic mobility in large grain size solution processed organic semiconductor thin films. Appl. Phys. Lett. **92**, 063302 (2008)
24. H.A. Becerril, M.E. Roberts, Z. Liu, J. Locklin, Z. Bao, High-performance organic thin-film transistors through solution-sheared deposition of small-molecule organic semiconductors. Adv. Mater. **20**, 2588–2594 (2008)
25. T. Uemura, Y. Hirose, M. Uno, K. Takimiya, J. Takeya, Very high mobility in solution-processed organic thin-film transistors of highly ordered [1]benzothieno[3,2-b]benzothiophene derivatives. Appl. Phys. Exp. **2**, 111501 (2009)
26. C.W. Sele, B.K.C. Kjellander, B. Niesen, M.J. Thornton, J.B.P.H. van der Putten, K. Myny, H. J. Wondergem, A. Moser, R. Resel, A.J.J.M. van Breemen, N. van Aerle, P. Heremans, J.E. Anthony, G.H. Gelinck, Controlled deposition of highly ordered soluble acene thin films: effect of morphology and crystal orientation on transistor performance. Adv. Mater. **21**, 4926–4931 (2009)
27. M.J. Kim, H.W. Heo, Y.K. Suh, C.K. Song, Morphology control of TIPS-pentacene grains with inert gas injection and effects on the performance of OTFTs. Org. Electron. **12**, 1170–1176 (2011)
28. Y. Toko, B.Y. Zhang, T. Sugiyama, K. Katoh, T. Akahane, Characteristics of liquid crystal display fabricated by alignment transcription method. Mol. Cryst. Liq. Cryst. **304**, 107–112 (1997)
29. K. Sueoka, H. Nakamura, Y. Taira, Improving the moving-image quality of TFT-LCDs, Digest of SID Symposium, pp. 203–206 (1997)
30. S.G. Kim, S.M. Kim, Y.S. Kim, H.K. Lee, S.H. Lee, G.-D. Lee, J.-J. Lyu, K.H. Kim, Stabilization of the liquid crystal director in the patterned vertical alignment mode through formation of pretilt angle by reactive mesogen. Appl. Phys. Lett. **90**, 261910 (2007)
31. Y. Momoi, M. Kwak, D. Choi, Y. Choi, K. Jeong, T.i Koda, O. Haba, K. Yonetake. Polyimide-free LCD by dissolving dendrimers. J. SID **20**(9), 486–492 (2012)
32. J.C. Meredith, A.P. Smith, A. Karim, E.J. Amis, Combinatorial materials science for polymer thin-film dewetting. Macromolecules **33**, 9747–9756 (2000)
33. M. Kimura, Japan Patent Unexam. Publ. No.2009-175247

34. M. Kimura, Progress of rubbing and non-rubbing techniques, in *Proceedings of the IMID'10*, pp. 185–186 (2010)
35. S.H. Lee, S.M. Kim, S.-T. Wu, Emerging vertical-alignment liquid-crystal technology associated with surface modification using UV-curable monomer. J. SID **17**, 551–559 (2009)
36. L.D. Landau, E.M. Lifshitz, *Fluid Mechanics* (Pergamon Press, New York, 1987)
37. M. Kimura, K. Honda, S. Yodogawa, K. Ohtsuka, T.N. Oo, K. Miyashita, H. Hirata, T. Akahane, Flexible LCDs fabricated with a slit coater: not requiring an alignment film. J. SID **20**, 633–639 (2012)
38. S.V. Patankar, *Numerical Heat Transfer and Fluid Flow* (Hemisphere, New York, 1980)
39. H. Sato, K. Miyashita, M. Kimura, T. Akahane Study of liquid crystal alignment formed using slit coater. Jpn J. Appl. Phys. **50**, 01BC16 (2011)
40. A.S. Sonin, N.A. Churochkina, Liquid crystals stabilized by polymer networks. Polym. Sci. A. **52**, 463 (2010)
41. K. Ohtsuka, Y. Nagataki, K. Goda, T.N. Oo, K. Miyashita, H. Hirata, M. Kimura, T. Akahane, Study of liquid crystal display fabricated using slit coater under two ultraviolet irradiation conditions. Jpn. J. Appl. Phys. **52**, 05DB04 (2013)
42. Y. Nagataki, T.N. Oo, T. Yamamoto, K. Miyashita, H. Hirata, M. Kimura, T. Akahane, Study of electro-optical properties of liquid crystal/reactive mesogen-coated liquid crystal display fabricated by slit coater. Liq. Cryst. **41**, 667–672 (2013)
43. T.J. Chen, K.L. Chu, Pretilt angle control for single-cellgap transflective liquid crystal cells. Appl. Phys. Lett. **92**, 091102 (2008)
44. B.Y. Liu, L.J. Chen, Role of surface hydrophobicity in pretilt angle control of polymer-stabilized liquid crystal alignment systems. J. Phys. Chem. C **117**, 13474–13478 (2013)
45. A. Goetz, M.K. Memmer, M. Bremer, A. Taugerbeck, K. Tarumi, D. Pauluth. Advanced liquid crystal materials for fast switching display modes, in *Proceedings of the IDW'08*, LCT6—3 (2008)
46. A. Goetz, A. Taugerbeck, G. Bernatz, K. Tarumi, Advanced liquid-crystal materials for the polymersustained vertically aligned (PS-VA) mode. Digest SID Symp. **41**, 718–720 (2010)
47. E.Y. Jeon, K.H. Kim, J.H. Lee, T.H. Yoon, Single cellgap transflective liquid crystal device created by controlling the pretilt angle using a liquid crystalline reactive monomer. Opt. Express **19**, 25617–25622 (2011)
48. R.A.M. Hikmet, C.D. Witz, Gel layers for inducing adjustable pretilt angles in liquid crystal systems. J. Appl. Phys. **70**, 1265–1269 (1991)
49. D.K. Yang. Polymer-stabilized liquid crystal displays, in *Progress in Liquid Crystal Science and Technology in Honor of Shunsuke Kobayashi's 80th Birthday,* ed. by H.S. Kwok, S. Naemura, H.L. Ong (World Scientific, 2013), pp. 597–628
50. A. Koike, M. Nishizawa, H. Tokunaga, J. Akiyama, T. Tsujimura, K. Hayashi, Novel non-alkaline glass substrate with ultra-low thermal shrinkage for higher resolution active matrix displays, in *Proceedings of the IDW'13*, FMC4-2 (2013)
51. N. Kooy, K. Mohamed, L.T. Pin, O.S. Guan, A review of roll-to-roll nanoimprint lithography. Nanoscale Res. Lett. **9**, 320–332 (2014)